2013-11-06

# *Structural Variation of Donor-Acceptor Copolymers Containing Benzodithiophene with Bithienyl Substituents to Achieve High Open Circuit Voltage in Bulk Heterojunction Solar Cells*

UTD AUTHOR(S): Ruvini Kularatne, Ferdinand Taenzler, Harsha Magurudeniya, Bruce Gnade, Michael Biewer and Mihaela Stefan

Journal of Materials Chemistry A

RSC Publishing

PAPER

View Article Online
View Journal | View Issue

Cite this: J. Mater. Chem. A, 2013, 1, 15535

# Structural variation of donor–acceptor copolymers containing benzodithiophene with bithienyl substituents to achieve high open circuit voltage in bulk heterojunction solar cells†

Ruvini S. Kularatne,[a] Ferdinand J. Taenzler,[a] Harsha D. Magurudeniya,[a] Jia Du,[a] John W. Murphy,[b] Elena E. Sheina,[c] Bruce E. Gnade,[b] Michael C. Biewer*[a] and Mihaela C. Stefan*[a]

Received 13th September 2013
Accepted 5th November 2013

DOI: 10.1039/c3ta13686h

www.rsc.org/MaterialsA

Three new donor–acceptor copolymers **P1**, **P2**, and **P3** were synthesized with benzodithiophene with bithienyl substituents as the donor and 5,6-difluorobenzo[*c*][1,2,5]thiadiazole, 4,7-di(thiophen-2-yl)-benzo[*c*][1,2,5]thiadiazole, and 5,6-difluoro-4,7-di(thiophen-2-yl)benzo[*c*][1,2,5]thiadiazole as the acceptors, respectively. The insertion of thiophene spacer between the donor and the acceptor broadened the absorption of the polymers **P2** and **P3** and resulted in a red shift of ~30 nm as compared to that of the polymer **P1**. However, the inclusion of fluorine atoms on the polymer had detrimental effects on the photovoltaic properties of the polymers. The synthesized donor–acceptor polymers were tested in bulk heterojunction (BHJ) solar cells with [6,6]-phenyl $C_{71}$ butyric acid methyl ester ($PC_{71}BM$) acceptor. Polymer **P2** gave a PCE of 3.52% with $PC_{71}BM$ in which the active layer was prepared in chloroform with 3% v/v 1,8-diiodooctane (DIO) additive. The effect of fluorine substitution and thiophene group insertion on the UV/Vis absorbance, photovoltaic performances, morphology, and charge carrier mobilities for the polymers are discussed.

## 1. Introduction

The low cost, light weight, flexibility, and easy processability on large area substrates make polymer solar cells promising candidates for renewable energy resources. Power conversion efficiencies (PCE) as high as 9.2% have been reported.[1,2] Extensive research has been performed in the past decade to improve the PCE of polymer solar cells in bulk heterojunction (BHJ) device architecture.[3–7] The active layer which is a blend of donor semiconductor polymers and fullerene acceptor of a bulk heterojunction solar cell (BHJ) plays a pivotal role. The short circuit current density ($J_{SC}$) and the open circuit voltage ($V_{OC}$) depend on the electronic properties of the active layer. A deeper highest occupied molecular orbital (HOMO) and a strong absorption overlapping the solar spectrum are desirable properties of donor semiconducting polymers which are expected to provide high $V_{OC}$ and $J_{SC}$, respectively. The benzodithiophene (BDT) donor–acceptor copolymers are in the forefront of the field of organic solar cells due to several advantages, such as a planar backbone and flexibility of attaching different substituents on the central benzene ring to fine tune the energy levels of the polymer.[4,8,9] Alkyl, alkoxy, thioalkyl, phenylethynyl, and thienyl substituted BDT have been synthesized by various research groups and PCEs as high as 7% have been achieved.[8–17]

Previously, our research group reported the synthesis of a bis(bithienyl)-substituted BDT as a donor for organic solar cells which gave a PCE of 2.52% with benzo[*c*][1,2,5]thiadiazole as the acceptor unit (Table S5 and Fig. S29 in ESI†).[18] The attachment of six alkyl substituents per BDT repeat unit was highly beneficial due to several advantages: (1) highly soluble polymers with very high molecular weights could be synthesized, (2) the insertion of alkyl chains on the acceptor units was deemed unnecessary, due to the solubilizing effect of the six alkyl substituents attached to BDT unit, and (3) the conjugated bithienyl substituents perpendicular to the polymer backbone provided a broader absorption in the visible region.

Benzo[*c*][1,2,5]thiadiazole has been widely used as a strong electron withdrawing acceptor moiety in D–A copolymers.[19–21] Recently, several groups have reported the insertion of thiophene spacer group in between the donor and acceptor moieties for efficient device performances in BHJ solar cells.[22–24] The insertion of the thiophene spacer groups relieved the steric

[a]Department of Chemistry, University of Texas at Dallas, 800 West Campbell Road, Richardson, TX 75080, USA. E-mail: mihaela@utdallas.edu; biewerm@utdallas.edu
[b]Department of Materials Science and Engineering, University of Texas at Dallas, 800 West Campbell Road, Richardson, Texas 75080, USA
[c]Plextronics. Inc, 2180 WilliamPitt Way, Pittsburgh, PA 15238, USA

† Electronic supplementary information (ESI) available: NMR Spectra, UV-vis Spectra, Cyclic Voltammograms, TGA thermograms, and 2D TMAFM phase images are included here. See DOI: 10.1039/c3ta13686h

hindrance between the acceptor and the donor units and hence the polymers had a planar polymer backbone.[19] This enhanced the conjugation along the polymer backbone, reduced the band gap, and improved the solid state packing and hence increased the $J_{SC}$ of the BHJ devices. The $V_{OC}$ of a BHJ solar cell device is largely determined by the HOMO level of the donor–acceptor (D–A) copolymer as the $V_{OC}$ is proportional to the energy difference between the HOMO level of the D–A copolymer and the LUMO level of the acceptor fullerene.[25] It has been demonstrated that the use of fluorine atom on the acceptor in D–A copolymers decreased the HOMO level and hence increased the $V_{OC}$ of the BHJ solar cell devices.[26–29] In addition, the smaller size of the fluorine atom as compared to other electron withdrawing groups such as trifluoromethyl groups and cyano groups has not imparted too much steric hindrance on the polymer backbone.[15]

Here we report the synthesis of three donor–acceptor polymers with bis(bithienyl)-substituted BDT as the donor unit and 5,6-difluorobenzo[*c*][1,2,5]thiadiazole, 4,7-di(thiophen-2-yl)-benzo[*c*][1,2,5]thiadiazole, and 5,6-difluoro-4,7-di(thiophen-2-yl)benzo[*c*][1,2,5]thiadiazole acceptors by Stille coupling polymerization. The effect of fluorine atom substitution and thiophene insertion on the photovoltaic properties of the D–A copolymers has been investigated.

## 2. Experimental section

### 2.1. Structural analysis

**NMR measurements.** $^1$H and $^{13}$C NMR spectra were recorded using Bruker Avance 500 MHz spectrometer at 25 °C or otherwise at indicated temperatures. The spectra were recorded in $CDCl_3$ or in toluene-$d_8$. The data are reported as follows: chemical shifts are reported in ppm on the $\delta$ scale relative to trimethylsilane (TMS) as the internal standard, multiplicity (br = broad, s = singlet, d = doublet, t = triplet, q = quartet, m = multiplet).

**GC–MS measurements.** GC–MS was obtained on an Agilent 6890-5973 GC/MS workstation. The GC column was a Hewlett-Packard fused silica capillary column cross-linked with 5% phenylmethylsiloxane. Helium was the carrier gas (1 mL min$^{-1}$). The following conditions were used for all GC/MS analysis: injector and detector temperature, 250 °C; initial temperature, 70 °C; temperature ramp, 10 °C min$^{-1}$; final temperature, 280 °C.

**Solid–liquid chromatography.** Analytical thin layer chromatography was performed on EM reagents 0.25 mm silica gel 60-F plates. Column chromatography was performed using the indicated solvent system on select silica gel ($SiO_2$) 230–400 mesh.

**Size exclusion chromatography.** The average molecular weights of the synthesized polymers were measured by size exclusion chromatography (SEC) analysis on a Varian PL-GPC 220 system equipped with Varian PL-Gel Mixed D column (300 mm × 7.5 mm, 5 μm) and Varian PL-Gel guard column (50 mm × 7.5 mm, 5 μm). A GPC solvent/sample module was used with chlorobenzene with 0.0125% BHT as the eluent and the calibrations were based on polystyrene standards. The running conditions for SEC analysis were as follows: flow rate = 1.0 mL min$^{-1}$, injector volume = 200 μL, detector temperature = 80 °C, column temperature = 80 °C. All the polymer samples were dissolved in chlorobenzene and the solutions were filtered through PTFE filters (0.45 μm) prior to injection.

### 2.2. Optoelectronic properties of the synthesized polymers

**UV-Vis measurements.** The UV-vis spectra of polymer solutions in chloroform solvent were carried out in 1 cm cuvettes using an Agilent 8453 UV-vis spectrometer. Thin films of polymer were obtained by evaporation of chloroform from polymer solutions on glass microscope slides. In order to measure absorption coefficient of the polymers, 5 mg mL$^{-1}$ polymer solutions were spin-coated at 600 rpm, 800 rpm and at 1000 rpm on pre-cleaned glass slides and the absorption were measured at the absorption maxima of each polymer. The film thickness for each glass slide was measured using a Veeco Dektak VIII profilometer.

**Cyclic voltammetry.** CV was obtained with a BAS CV-50 W Voltammetric Analyzer (Bioanalytical Systems, Inc.). Electrochemical grade tetrabutylammonium perchlorate (TBAP) was used without further purification. Acetonitrile was distilled over calcium hydride and collected over molecular sieves. The electrochemical cell was comprised of a platinum electrode, a platinum wire auxiliary electrode and an Ag/AgCl reference electrode. Acetonitrile solutions containing 0.1 M TBAP were placed in a cell and purged with argon. A drop of the polymer solution was evaporated in ambient air. The film was immersed into the electrochemical cell containing the electrolyte and the oxidation potential was observed and recorded. All electrochemical shifts were standardized to the ferrocene redox couple at 0.474 V.

**Preparation of solar cell devices.** Glass substrates coated with ITO were purchased from Luminescence Technology Corp. (Taiwan) and were patterned using standard photolithography. The substrates were cleaned by sonication for 20 minutes in acetone, methanol, toluene, and isopropyl alcohol. The substrates were subjected to UV/ozone treatment for 20 minutes prior to use. After the ozone treatment, poly(3,4-ethylenedioxythiophene):poly(styrenesulfonate) PEDOT:PSS was spin coated on the substrates (4000 rpm, 1740 rpm s$^{-1}$, 90 s). The substrates were annealed at 150 °C for 10 minutes under a nitrogen atmosphere. Polymer/PCBM blends were prepared in chloroform with a total blend concentration of 15 mg mL$^{-1}$. For the solar cells with 1,8-diiodooctane (DIO) additive, the blends were prepared by adding DIO dissolved in chloroform to a polymer/PCBM blend such that the total concentration was 15 mg mL$^{-1}$. These blends were spin coated (2000 rpm, 1740 rpm s$^{-1}$, 60 s) on to the PEDOT:PSS treated substrate. Films of 20 nm Ca and 100 nm Al were thermally evaporated on to the substrates at a rate of 2.75 Å s$^{-1}$ through a shadow mask to obtain the solar cell devices.

IV testing was carried out under a controlled nitrogen atmosphere using a Keithley 236, model 9160 interfaced with LabView software. The solar simulator used was a

 

THERMOORIEL equipped with a 300 W Xenon lamp; the intensity of the light was calibrated to 100 mW $cm^{-2}$ with a NREL certified Hamamatsu silicon photodiode. The active area of the devices was 0.1 $cm^2$. The active layer film thickness was measured using a Veeco Dektak VIII profilometer.

**Space charge limited current measurements.** ITO patterned glass substrates were cleaned by sonication for 20 minutes in acetone, methanol, toluene, and isopropyl alcohol. The substrates were subjected to UV/ozone treament for 20 minutes prior to use. After the ozone treatment, poly(3,4-ethylenedioxythiophene):poly(styrenesulfonate) PEDOT:PSS was spin coated on the substrates (4000 rpm, 1740 rpm $s^{-1}$, 90 s). The substrates were annealed at 150 °C for 10 minutes under a nitrogen atmosphere. Polymer solutions (15 mg $mL^{-1}$ concentration) were prepared in chloroform and were spin coated (2000 rpm, 1740 rpm $s^{-1}$, 60 s) on to PEDOT:PSS treated substrate. Aluminum (100 nm thickness) was thermally evaporated on the substrates at a rate of 2.75 Å $s^{-1}$ through a shadow mask to obtain the solar cell devices.

IV testing was carried out under a controlled nitrogen atmosphere using a Keithley 236, model 9160 interfaced with LabView software. The active area of the devices was 0.1 $cm^2$. The active layer film thickness was measured using a Veeco Dektak VIII profilometer.

**Tapping Mode Atomic Force Microscopy (TMAFM).** Tapping Mode Atomic Force Microscopy (TMAFM) was carried out on the active area of the solar cell devices and on the area in between the channels of the OFET devices. AFM studies were carried out on a VEECO-dimension 5000 scanning probe microscope with a hybrid *xyz* head equipped with Nano-Scope Software. AFM images were obtained using silicon cantilevers with nominal spring constant of 42 N $m^{-1}$ and nominal resonance frequency of 300 kHz (OTESPa). Image analysis software Nanoscope 7.30 was used for surface imaging and image analysis. All the AFM measurements were taken of the active area of solar cell devices and were conducted under ambient conditions. All cantilever oscillation amplitude was equal to *ca.* 375 mV, and all images were acquired at 2 Hz scan frequency. Sample scan area was 5 μm.

### 2.3. Synthesis of the monomers and polymers

The monomers 1 to 6 were synthesized according to previously reported procedures with slight modifications in each step.[30,31]

**Synthesis of 4,5-difluorobenzene-1,2-diamine (1).** 4,5-Difluoro-2-nitroaniline (5.00 g, 0.0288 mol) was dissolved in concentrated HCl (150 mL). At 0 °C tin (16.56 g, 0.140 mol) was added in small portions over 15 minutes. The reaction mixture was stirred at room temperature until all the tin was dissolved, and was further stirred for another one hour after which it was refrigerated overnight. The reaction mixture was poured into deionized water and a solution of NaOH (4 M) was added gradually until the solution reached pH 10. The organic phase was extracted with ethyl acetate (4 × 100 mL), washed with water (4 × 100 mL), and dried over anhydrous $MgSO_4$. The solution was concentrated in vacuum to obtain 2.98 g of pink crystals. (0.0207 mol, 72%). $^1$H NMR (500 MHz, $CDCl_3$): $\delta_H$ 6.50 (t, 2H), 3.24 (s, 4H).

**Synthesis of 5,6-difluorobenzo[*c*][1,2,5]thiadiazole (2).** 4,5-Difluorobenzene-1,2-diamine (3.30 g, 0.0229 mol) and triethylamine (12.87 mL, 0.0916 mol) were dissolved in chloroform (300 mL) under a nitrogen atmosphere and the reaction mixture was stirred until all the 4,5-difluorobenzene-1,2-diamine was dissolved. Thionyl chloride ($SO_2Cl$) (5.94 mL, 0.0503 mol) was added drop-wise and the reaction mixture was refluxed for 3 days. The reaction mixture was cooled to room temperature and the organic phase was extracted with methylene chloride (3 × 100 mL), washed with water (3 × 100 mL), and dried over anhydrous $MgSO_4$. Evaporation of the solvent generated 3.03 g of product as brown needle-like crystals (0.0176 mol, 77%). $^1$H NMR (500 MHz, $CDCl_3$): $\delta_H$ 7.75 (t, 2H).

**Synthesis of 5,6-difluoro-4,7-bis(trimethylsilyl)benzo[*c*][1,2,5]thiadiazole (3).** Freshly distilled diisopropylamine (6.06 mL, 0.0424 mol) was diluted with THF (40 mL) under a nitrogen atmosphere and at −78 °C and 2.5 M *n*-BuLi in hexane (16.4 mL, 0.0409 mol) was added drop-wise to the reaction mixture. The reaction mixture was stirred for 2 h at −78 °C at which time the synthesized lithium diisopropylamine (LDA) was cannulated to a three neck flask containing the 5,6-difluorobenzo[*c*][1,2,5]thiadiazole (3.2 g, 0.0186 mol) in THF (80 mL) at −78 °C. After the addition, the reaction was stirred for 30 min at −78 °C, followed by the drop-wise addition of trimethylsilylchloride (5.58 mL, 0.0436 mol). The reaction mixture was stirred at −78 °C for 3 h. A saturated solution of $NH_4Cl$ (10 mL) was added to the reaction mixture which was allowed to warm up to room temperature for 1 h. An additional portion of saturated $NH_4Cl$ was added and the organic phase was extracted with chloroform (3 × 100 mL), washed with water (5 × 100 mL), and dried over anhydrous $MgSO_4$. The solvent was removed in vacuum to obtain a brown oil, which was further purified by column chromatography using hexane as the eluent to obtain 1.76 g of colorless oil (0.00558 mol, 30%). $^1$H NMR (500 MHz, $CDCl_3$): $\delta_H$ 0.52 (s, 18H). $^{13}$C NMR (125 MHz, $CDCl_3$): $\delta_C$ 0.07, 117.0 (t), 154.6 (t), (158.0, 156.0 (dd)).

**Synthesis of 4,7-dibromo-5,6-difluorobenzo[*c*][1,2,5]thiadiazole (4).** 5,6-Difluoro-4,7-bis(trimethylsilyl)benzo[*c*][1,2,5]thiadiazole (2.0 g, 0.00633 mol) was added to a three neck flask and it was diluted with chloroform (30 mL). When the 5,6-difluoro-4,7-bis(trimethylsilyl)benzo[*c*][1,2,5]thiadiazole was dissolved completely, bromine (19.68 mL, 0.0127 mol) was added to the reaction mixture and the reaction was stirred for 2 days at 60 °C in dark. The reaction mixture was then cooled to room temperature and it was quenched in 4 M NaOH solution. The organic phase was extracted with chloroform and was washed with brine (3 × 100 mL), water (3 × 100 mL), and dried over anhydrous $MgSO_4$. The solvent was evaporated to obtain a white solid which was further purified by column chromatography using hexanes as the eluent to obtain 0.627 g of white needle-like crystals (0.001899 mol, 30%).$^{13}$C NMR (125 MHz, $CDCl_3$): $\delta_C$ 99.40 (t), 148.8 (t), (150.6, 152.8 (dd)).

**Synthesis of 5,6-difluoro-4,7-di(thiophen-2-yl)benzo[*c*][1,2,5]thiadiazole (5).** 4,7-Dibromo-5,6-difluorobenzo[*c*][1,2,5]thiadiazole (0.360 g, 0.00109 mol), 2-(tributylstannyl) thiophene

(0.720 mL, 0.00226 mol) and tetrakis(triphenylphosphine)-palladium(0) (43.5 mg, $4.35 \times 10^{-5}$ mol) were added to a three neck flask under a nitrogen atmosphere and was dissolved in a mixture of toluene (20 mL) and DMF (0.5 mL). The reaction mixture was refluxed for 12 h at which time a sample was taken to determine the monomer conversion. When there was no starting material left in the reaction mixture the reaction was cooled and potassium fluoride (6 g) in water (10 mL) was added to the reaction and it was stirred for 2 h. The reaction mixture was quenched in ice cold water (100 mL) and the organic phase was extracted with methylene chloride (3 × 100 mL). The organic phase was washed with 10% HCl (3 × 100 mL), saturated $NaHCO_3$ (3 × 100 mL), and dried over anhydrous $MgSO_4$. The solvent was evaporated in vacuum to obtain a yellow solid, which was further purified by column chromatography using 99 : 1 hexanes : ethyl acetate as the eluent to obtain 0.146 g of bright yellow needle like crystals. (0.000436 mol, 40%). $^1$H NMR (500 MHz, $CDCl_3$): $\delta_H$ 7.27 (t, 2H), 7.61(d, 2H), 8.29 (d, 2H). $^{13}$C NMR (125 MHz, $CDCl_3$): $\delta_C$ 111.0 (t), 127.5, 129.0, 131.0, 131.6, 148.8, (149.0, 151.0 (dd)).

**Synthesis of 4,7-bis(5-bromothiophen-2-yl)-5,6-difluorobenzo-[*c*][1,2,5]thiadiazole (6).** 5,6-Difluoro-4,7-di(thiophen-2-yl)benzo[*c*]-[1,2,5]thiadiazole (0.180 g, 5.85 × 10-4 mol) was dissolved in a mixture of chloroform (20 mL) and acetic acid (20 mL). At 0 °C, NBS (0.219 g, 0.00123 mol) was added slowly to the reaction mixture. After 1 hour an orange color compound precipitated. And the reaction was quenched in water (100 mL) and the organic phase was extracted into chloroform (3 × 100 mL). The organic phase was washed with water (3 × 100 mL) dried over anhydrous $MgSO_4$. The solvent was evaporated in vacuum to obtain 0.231 g of orange crystals ($4.66 \times 10^{-4}$ mol, 80%). $^1$H NMR (500 MHz, Toluene-d8): $\delta_H$ 6.83 (d, 2H), 7.78(d, 2H). $^{13}$C NMR (125 MHz, Toluene-d8): $\delta_C$ 111.5 (t), 117.6, 130.5, 131.46, 134.0, 148.6, (149.0, 150.1 (dd)).

**General procedures for the synthesis of polymers P1, P2 and P3 through Stille coupling polymerization**

*Synthesis of poly{4-(4,8-bis(3,3′,5′-trihexyl-2,2′-bithiophen-5-yl)-benzo[1,2-b:4,5-b′]dithiophen-2-yl)-alt-5,6-difluorobenzo[c][1,2,5]-thiadiazole} (**P1**).* 4,7-Dibromo-5,6-difluorobenzo[*c*][1,2,5]thiadiazole (98.2 mg, $2.964 \times 10^{-4}$ mol), (4,8-bis(3,3′,5′-trihexyl-2,2′-bithiophen-5-yl)benzo[1,2-b:4,5-b′]dithiophene-2,6-diyl)bis(trimethylstannane) (403 mg, $2.986 \times 10^{-4}$ mol) and tetrakis-(triphenylphosphine)palladium(0) (9.97 mg, $9.80 \times 10^{-6}$ mol) were added to a three neck flask under a nitrogen atmosphere. The compounds were dissolved in a mixture of toluene (20 mL) and DMF (0.5 mL) and were refluxed at 110 °C for 12 hours, at which time the reaction temperature was decreased to 100 °C and was diluted with toluene (40 mL). The polymerization was stopped after 24 h by precipitating the polymer in a mixture of methanol (300 mL) and HCl (30 mL). The polymer was purified by Soxhlet extractions with methanol, hexane, ether and chloroform with successive drying between each extraction. A dark blue polymer was obtained by the evaporation of the chloroform extract. (0.120 g, 35% yield). $^1$H NMR (500 MHz, $CDCl_3$): $\delta_H$ 0.88 (br, 6H), 0.99 (br, 12H), 1.26 (br, 56H), 1.43, (br (12H), 1.55 (br, 12H), 2.72 (t, 8H), 2.84 (t, 4H), 6.74 (s, 2H), 8.50 (s, 2H), 9.52 (s, 2H).

*Synthesis of poly{4-(4,8-bis(3,3′,5′-trihexyl-2,2′-bithiophen-5-yl)-benzo[1,2-b:4,5-b′]dithiophen-2-yl)-alt-4,7-di(thiophen-2-yl)benzo-[c][1,2,5]thiadiazole} (**P2**).* Using a procedure similar to that described above for the polymer **P1**, a mixture of 4,7-bis(5-bromothiophen-2-yl)benzo[*c*][1,2,5]thiadiazole (103.2 mg, $2.18 \times 10^{-4}$ mol),[30] (4,8-bis(3,3′,5′-trihexyl-2,2′-bithiophen-5-yl)benzo-[1,2-*b*:4,5-*b*′]dithiophene-2,6-diyl)bis(trimethylstannane) (304 mg, $2.18 \times 10^{-4}$ mol) and tetrakis(triphenylphosphine)palladium (0) (7.50 mg, $7.266 \times 10^{-6}$ mol) in dry toluene was polymerized to generate polymer **P2.** (100 mg, 35% yield). $^1$H NMR (500 MHz, $CDCl_3$): $\delta_H$ 0.92 (br, 18H), 1.53 (br, 56H), 1.81 (br, 24H) 2.70 (t, 8H), 2.90 (t, 4H), 6.79 (s, 2H), 7.53 (s, 2H), 7.70 (s, 2H), 7.86 (s, 2H).

*Synthesis of poly{4-(4,8-bis(3,3′,5′-trihexyl-2,2′-bithiophen-5-yl)-benzo[1,2-b:4,5-b′]dithiophen-2-yl)-alt-4,7-di(thiophen-2-yl)-5,6-di(fluoro)benzo[c][1,2,5]thiadiazole} (**P3**).* Using a procedure similar to that described above for the polymer **P1**, a mixture of 4,7-bis(5-bromothiophen-2-yl)-5,6-difluorobenzo[*c*][1,2,5]thiadiazole (122 mg, $2.48 \times 10^{-4}$ mol), (4,8-bis(3,3′,5′-trihexyl-2,2′-bithiophen-5-yl)benzo[1,2-*b*:4,5-*b*′]dithiophene-2,6-diyl)bis(trimethylstannane) (335 mg, $2.48 \times 10^{-4}$ mol) and tetrakis-(triphenylphosphine)palladium(0) (8.39 mg, $8.266 \times 10^{-6}$ mol) in dry toluene was polymerized to generate polymer **P3**. (100 mg, 30% yield). $^1$H NMR (500 MHz, $CDCl_3$): $\delta_H$ 0.92 (br, 18H), 1.53 (br, 56H), 1.81 (br, 24H) 2.70 (t, 8H), 2.90 (t, 4H), 6.70 (s, 2H), 7.70 (s, 2H), 7.91 (s, 2H), 8.20 (s, 2H).

## 3. Results and discussion

### 3.1. Synthesis

Three alternating donor–acceptor polymers have been synthesized by Stille coupling polymerization using (4,8-bis(3,3′,5′-trihexyl-2,2′-bithiophen-5-yl)benzo[1,2-*b*:4,5-*b*′]dithiophene-2,6-diyl)bis(trimethylstannane)as the donor monomer. Equimolar quantities of (4,8-bis(3,3′,5′-trihexyl-2,2′-bithiophen-5-yl)benzo-[1,2-*b*:4,5-*b*′]dithiophene-2,6-diyl)bis(trimethylstannane) were reacted with 4,7-dibromo-5,6-difluorobenzo[*c*][1,2,5]thiadiazole, 4,7-bis(5-bromothiophen-2-yl)benzo[*c*][1,2,5]thiadiazole, and 4,7-bis(5-bromothiophen-2-yl)-5,6-difluorobenzo[*c*][1,2,5]-thiadiazole (Scheme 1 and S1 in the ESI†) in the presence of tetrakis(triphenylphosphene)palladium(0) catalyst. The synthesis of polymers **P1**, **P2** and **P3** is shown in Scheme 2. The

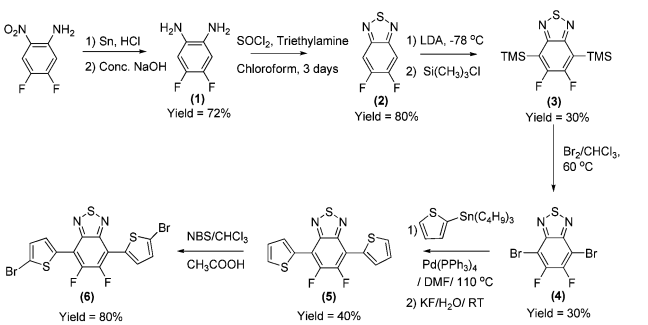


**Scheme 1** Synthesis of 4,7-bis(5-bromothiophen-2-yl)-5,6-difluorobenzo[*c*]-[1,2,5]thiadiazole

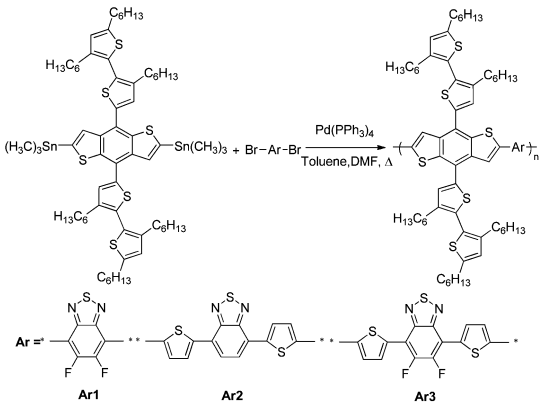


**Scheme 2** Synthesis of the donor–acceptor polymers **P1**, **P2** and **P3**.

SEC analysis was used to determine the molecular weights of the polymers. The estimated molecular weights had values ranging from 20 000 g $mol^{-1}$ to 28 000 g $mol^{-1}$ (Table 1).

The synthesized polymers had relatively broad polydispersity index (PDI) which are due to the *non-living* nature of the Stille coupling polymerization. Polymers **P1**, **P2**, and **P3** had good solubility in common organic solvents such as chloroform, toluene, and chlorobenzene. The polymers were characterized by $^1$H NMR and the $^1$H NMR spectra of the reported polymers are shown in (ESI†).

### 3.2. UV-Vis spectroscopy

The UV-vis absorption spectra were recorded for the polymers **P1**–**P3** in chloroform solution and in thin films obtained by the drop-casting the chloroform solutions onto glass substrates (Table 1, Fig. S19 in ESI†). Polymers **P2** and **P3** showed two absorption maxima, one at 350 nm and the second one in the visible region (> 550 nm), whereas polymer **P1** showed several absorption maxima bands, among which the most prominent bands with very high intensity are at ~350 nm and ~650 nm. The strong absorption peaks in the visible region (~653 nm for polymer **P1**, ~621 nm for polymer **P2** and ~615 nm for polymer **P3**) are due to the π–π* transition along the conjugated polymer backbone.[17,32] The absorption maxima observed in the UV region (~343 nm for polymer **P1**, ~374 nm for polymer **P2** and ~368 nm for polymer **P3**) is due to the conjugation along the side chain of the benzodithiophene moiety. Both polymers **P2** and **P3** showed a red-shift (~28 nm for polymer **P2** and ~13 nm for polymer **P3**) in absorption bands of polymer thin films compared to that of the solutions. However, polymer **P1** did not show any red-shift in the absorption bands of the polymer thin films as compared to that of the solution. The absence of a red-shift was attributed to the fact that the polymer **P1** has a rigid rod conformation both in solution and thin films.[33,34] The red-shift in absorption maxima in thin films compared to that of the solution, for the polymer **P2** and **P3** indicated more structural organization and ordered packing which enhanced the aggregation of the polymer in thin films compared to that of the solution. The incorporation of thiophene spacer in between the donor and the acceptor in the polymers **P2** and **P3**, may result in a less rigid and planar structure in solution due to the twisting of the polymer chain and this may be prevented in solid state resulting in ordered packing, enhanced conjugation and π-delocalization hence a red shift in thin films.[35] The onset of absorption for the polymer **P1** was 725 nm, for polymer **P2** was 737 nm and for the polymer **P3** was 750 nm corresponding to optical band gaps of 1.71 eV, 1.69 eV, and 1.65 eV, respectively.

The absorption coefficients of the polymers were determined by spin coating polymer solutions on glass substrates at different spin rates (1000 rpm, 800 rpm and 600 rpm) to obtain different film thicknesses. The absorption coefficients of these polymer films were calculated at the maximum absorption of the polymers. Table S1 in ESI† summarizes the absorption coefficients obtained for the polymers at different polymer film thicknesses. The absorbance coefficient for all the polymers decreased with the increasing the thickness of the polymer film.

### 3.3. Cyclic voltammetry

The HOMO and LUMO energy levels of the polymers were determined by cyclic voltammetry using $Ag/Ag^+$ non-aqueous electrode as the reference electrode as well as using the photoelectron spectroscopy. For the cyclic voltammetric measurements the HOMO and LUMO energy levels for the polymers were calculated by using the following equations: HOMO = $-[E_{ox} + 4.71]$ eV; LUMO = $-[E_{red} + 4.71]$ eV, where the $E_{ox}$ and $E_{red}$ are the onset of oxidation and reduction potentials respectively (Fig. S20, ESI†). The HOMO levels of the polymers measured from cyclic voltammetry and that from photoelectron spectroscopy showed similar trends (Table 1).

Polymer **P1** had a HOMO level of −5.64 eV while polymer **P3** had a HOMO energy level of −5.52 eV. By contrast, polymer **P2** had a higher HOMO energy level of −5.47 eV. This was attributed to the incorporation of electron withdrawing fluorine substituents to the conjugated polymer backbone which decreased the HOMO level of polymers **P1** and **P3**.[15] Both

**Table 1** Molecular weight, optical and electronic energy levels of **P1**, **P2**, **P3**

| Polymer | $M_n$[a] ($gmol^{-1}$) | PDI | HOMO[b] (eV) | LUMO[c] (eV) | $E_g$[d] (eV) | HOMO[e] (eV) | $\lambda_{max}$[f] (nm) | $\lambda_{max}$[g] (nm) |
|---|---|---|---|---|---|---|---|---|
| **P1** | 22 600 | 1.8 | −5.64 | −3.39 | 2.25 | −5.57 | 343, 494, 593, 653 | 343, 494, 595, 656 |
| **P2** | 28 097 | 2.9 | −5.47 | −3.13 | 2.34 | −5.29 | 374, 590, 621 | 393, 606, 649 |
| **P3** | 20 100 | 2.9 | −5.52 | −3.15 | 2.37 | −5.40 | 368, 579, 615 | 377, 598, 628 |

[a] Determined by SEC (chlorobenzene eluent). [b] Estimated from the onset of oxidation wave of cyclic voltammogram. [c] Estimated from the onset of reduction wave of cyclic voltammograms. [d] $E_g$=(LUMO[c]–HOMO[b]). [e] Estimated from the AC2 measurements. [f] Absorption maxima of chloroform solution. [g] Absorption maxima of thin films.

polymers **P2** and **P3** have a 0.2 eV difference in their HOMO and LUMO values compared to that of the HOMO and LUMO energy levels of the polymer **P1** which was attributed to the more extended conjugation and the π-electron delocalization arising from the incorporation of thiophene spacer in between the donor and the acceptor moieties. All reported polymers have deep lying HOMO energy levels which are lower than the air oxidation threshold (*ca.* −5.27 eV) indicating good air stability.[36,37] Moreover, due to the lower HOMO energy level of these polymers a higher $V_{OC}$ for BHJ could be potentially obtained.[25]

### 3.4. Thermogravimetric analysis

The thermal stability of the polymers was investigated using thermogravimetric analysis (TGA) under a nitrogen atmosphere with a heating rate of 10 °C $min^{-1}$ (Fig. S21 in ESI†). The onset of decomposition temperature for all the three polymers **P1**, **P2** and **P3** is above 400 °C indicating good thermal stability.

### 3.5. Bulk heterojunction (BHJ) solar cell studies

The photovoltaic properties of the polymers were investigated for the polymers **P1**, **P2** and **P3** in bulk heterojunction solar cell using $PC_{71}BM$ as the acceptor. The solar cells were fabricated with a device structure of ITO/PEDOT:PSS/Polymer: $PC_{71}BM$/Ca/Al with a device area of 0.1 $cm^2$ for the polymers **P1**, **P2** and **P3** and were tested under AM 1.5 AMG illuminations.

In order to maintain a constant active layer thickness for the solar cell devices of the polymers a total blend concentration of 15 mg $mL^{-1}$ in chloroform was maintained and the polymer blend was spin-casted at a spin rate of 2000 rpm on ITO substrates that have been treated with PEDOT: PSS. The effect of $PC_{71}BM$ on the photovoltaic properties of the polymers were investigated by varying the blend ratio of polymer: $PC_{71}BM$ from 1 : 1 to 1 : 4 (Table 2).

Polymer **P2** with 4,7-di(thiophen-2-yl)benzo[*c*][1,2,5]thiadiazole as the acceptor unit gave the highest PCE of 2.96% ($V_{OC}$ = 0.91 V, FF = 0.42 and $J_{SC}$ = 7.90 mA $cm^{-2}$) for the polymer: $PC_{71}BM$ 1 : 1 weight ratio. The PCE of polymer **P2** decreased with increasing the $PC_{71}BM$ weight ratio and a decrease in the open circuit voltage ($V_{OC}$) was also observed. The polymer **P3** with 5,6-difluoro-4,7-di(thiophen-2-yl)benzo[*c*][1,2,5]thiadiazole as the acceptor moiety gave a PCE of 2.67% ($V_{OC}$ = 0.90 V, FF = 0.37 and $J_{SC}$ = 8.03 mA $cm^{-2}$) for the polymer : $PC_{71}BM$ 1 : 1 weight ratio. The short circuit current density ($J_{SC}$) and the PCE of the polymer **P3** decreased with the increase in $PC_{71}BM$ weight ratio. The polymer **P1** gave a lower PCE of 1.19% for the weight ratio of polymer: $PC_{71}BM$ 1 : 1 ($V_{OC}$ = 0.96 V, FF = 0.39 and $J_{SC}$ = 3.20 mA $cm^{-2}$). A similar trend was observed for polymer **P1** as compared to polymers **P2** and **P3** upon increasing the $PC_{71}BM$ weight ratio. All polymers gave exceptionally high $V_{OC}$ which was attributed to the low lying HOMO levels of the polymers (HOMO < −5.2 eV) as the $V_{OC}$ is related to the energy difference between the HOMO the polymer and the LUMO of the acceptor.[25] The insertion of fluorine atom on the acceptor decreased the HOMO and the LUMO levels of the polymers **P1** and **P3** as compared to the polymer **P2**.

Although the deeper HOMO levels are beneficial for the $V_{OC}$, due to the large band gap the excitons diffusion may be hindered and may also increase the charge recombination which in turn will decrease the short circuit current $J_{SC}$ of the device. This may be the reason for the lower $J_{SC}$ values and lower PCE measured for the polymer **P1**. It can be observed that the insertion of the thiophene spacer had a significant influence on solar cell performance. A two fold increase in $J_{SC}$ was observed for the polymers **P2** and **P3** as compared to polymer **P1**. This was attributed to the increased conjugation and enhanced absorption due to the thiophene spacer. However, the presence of fluorine had a negative effect on the device performance as polymer **P3** had lower PCE as compared to **P2**.

We attempted to further optimize the BHJ performance by using 1,8-diiodooctane (DIO) as a processing additive for the polymer–$PC_{71}BM$ blend (Table 3, Fig. 1, S22, S23 and S24 in ESI†). This high boiling point solvent (DIO) can selectively dissolve fullerene components in the polymer blend and thereby can affect the morphology of the active layer.[38] However, the effect of DIO as an additives on the solar cell device performance depends on the structure of the polymer and can

**Table 2** Photovoltaic properties of the **P1**, **P2** and **P3** in solar cell devices[a]

| Polymer | [P]:$PC_{71}BM$ | $V_{OC}$ (V) | $J_{SC}$ (mA $cm^{-2}$) | FF | PCE (%) | Thickness (nm) |
|---|---|---|---|---|---|---|
| **P1** | 1 : 1 | 0.96, (0.92) | 3.20, (3.14) | 0.39, (0.36) | 1.19, (1.06) | 81.44 |
| | 1 : 2 | 0.94, (0.90) | 2.97, (2.98) | 0.33, (0.32) | 0.92, (0.88) | 77.13 |
| | 1 : 3 | 0.78, (0.70) | 2.80, (2.82) | 0.30, (0.30) | 0.64, (0.59) | 83.91 |
| | 1 : 4 | 0.29, (0.23) | 2.60, (2.61) | 0.29, (0.29) | 0.22, (0.17) | 80.52 |
| **P2** | 1 : 1 | 0.91, (0.85) | 7.90, (8.33) | 0.42, (0.40) | 2.96, (2.84) | 87.89 |
| | 1 : 2 | 0.84, (0.79) | 7.78, (7.41) | 0.36, (0.32) | 2.34, (1.94) | 80.71 |
| | 1 : 3 | 0.73, (0.75) | 7.54, (7.01) | 0.36, (0.32) | 1.99, (1.73) | 84.89 |
| | 1 : 4 | 0.67, (0.66) | 7.66, (6.51) | 0.38, (0.37) | 1.94, (1.64) | 77.07 |
| **P3** | 1 : 1 | 0.90, (0.91) | 8.03, (7.81) | 0.37, (0.37) | 2.67, (2.61) | 79.11 |
| | 1 : 2 | 0.89, (0.87) | 6.16, (6.14) | 0.47, (0.43) | 2.60, (2.37) | 79.71 |
| | 1 : 3 | 0.89, (0.89) | 5.49, (5.48) | 0.50, (0.48) | 2.48, (2.36) | 83.57 |
| | 1 : 4 | 0.89, (0.89) | 5.62, (5.45) | 0.47, (0.46) | 2.38, (2.23) | 75.65 |

[a] Data in the parenthesis represents the average measured PCE values.

**Table 3** Photovoltaic properties **P1**, **P2** and **P3** with 3% DIO as an additive in solar cell devices[a]

| Polymer | $V_{OC}$ (V) | $J_{SC}$ (mA cm$^{-2}$) | FF | PCE (%) | Thickness (nm) |
|---|---|---|---|---|---|
| **P1** | 0.55, (0.44) | 3.19, (3.22) | 0.29, (0.29) | 0.51, (0.41) | 79.97 |
| **P2** | 1.03, (0.85) | 7.05, (8.22) | 0.48, (0.49) | 3.52, (3.43) | 78.37 |
| **P3** | 0.86, (0.86) | 7.72, (7.57) | 0.43, (0.43) | 2.93, (2.82) | 85.05 |

[a] Data in the parenthesis represents the average measured PCE values.

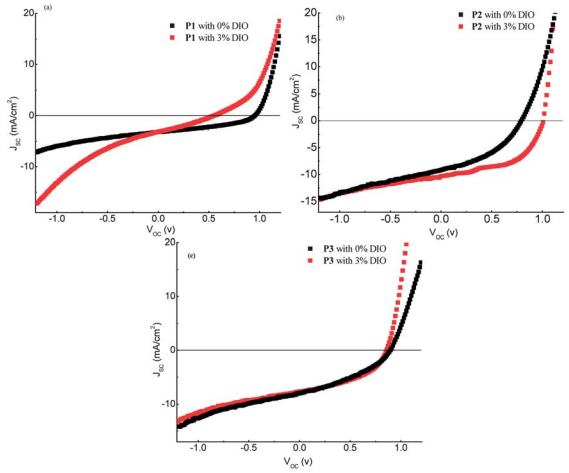


**Fig. 1** *J–V* curves for polymers **P1**, **P2** and **P3**.

either enhance[39–41] or decrease[11,42,43] the efficiency of the BHJ devices. For the polymers **P1**, **P2** and **P3** the DIO concentration was progressively increased from 1 to 5% v/v. The BHJ devices were fabricated with the same set of conditions used to obtain the highest PCEs for each polymer. For the polymer **P1**, addition of DIO had a detrimental effect on the $J_{SC}$, fill factor as well as on $V_{OC}$, thereby reducing the overall device performance (Table 3and S2 in ESI†). Previous work in our group has also shown that upon the addition of DIO as an additive decreased the device performance of the polymer(Table S5, S6 and Fig. S29 in ESI†).[18] For the polymers **P2** and **P3** an optimal DIO concentration of 3% v/v was used to obtain an increase in the PCE of the BHJ devices. Polymer **P2** gave the highest PCE of 3.52% with an impressive open circuit voltage of 1.03 V (FF = 0.48 and $J_{SC}$ = 7.04 mA cm$^{-2}$) for 3% (v/v) DIO content (Table 3 and S3 in ESI†). A similar trend was observed for the polymer **P3** in which the highest PCE of 2.93% was obtained with a $V_{OC}$ = 0.86 V, FF = 0.43 and a $J_{SC}$ = 7.72 mA cm$^{-2}$ for 3% (v/v) DIO content (Table 3, S4 in ESI†). For polymers **P2** and **P3** the fill factor increased with increasing the DIO concentration which could be attributed to the fact that upon the addition of DIO the phase separation was improved which in turn enhanced the charge transport and decreased the recombination losses.

### 3.6. Tapping Mode Atomic Force Microscopy (TMAFM) analysis

To investigate the differences in the efficiencies of the reported polymers the morphology of the active layer of the BHJ devices were investigated using tapping mode atomic force microscopy (TMAFM). It has been observed that smoother surface and a good phase separation are critical for good device performances as a smoother surface induces better contact with the electrode and the bicontinuous phase separation influence better charge transport and excitons dissociation.[18,44] The polymers with thiophene spacers (**P2** and **P3**) showed improved morphology with less surface roughness and better phase separation compared to the polymer **P1**, for which the PCBM and the polymer phase segregated and formed large domains. Presumably these larger domains may be PCBM (Fig. 2, S25 and S26 in ESI†). The active layer of the polymer **P2** showed a very smooth surface with an rms of 1.15 nm and the polymer **P3** had an rms of 1.22 nm. However, the active layer of polymer **P1** had a much less smooth surface and had an rms of 1.46 nm. Thus, the smoother morphology of the active layer of **P2** and **P3** seemed to aid the charge transport resulting in a better device performance. However, the higher surface roughness and the aggregation observed in the active layer of the polymer **P1** reflected in the poor device performance of the BHJ device.

TMAFM analysis was also performed for the solar cell devices of **P1**, **P2**, and **P3** with 3% DIO additive. A comparison of the TMAFM images of **P2**/$PC_{71}BM$ blend with 0% and 3% DIO indicated that upon the addition of DIO a very smooth active layer morphology was obtained (polymer **P2**: rms = 0.877 nm) which improved the device performance. The surface roughness of the polymer **P3** remained almost the same upon the addition of DIO which reflected in a very slight increase of PCE. However, for polymer **P1** the addition of DIO increased the surface

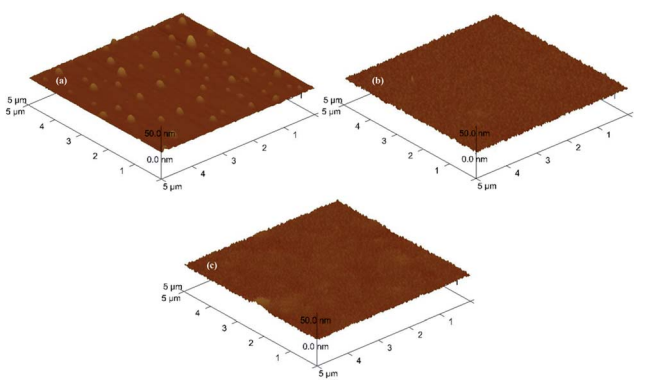


**Fig. 2** 3D TMAFM phase images of the solar cell devices without DIO: (a) polymer **P1** : $PC_{71}BM$ = 1 : 1blend (rms = 1.46 nm); (b) polymer **P2** : $PC_{71}BM$ = 1 : 1 blend (rms = 1.15 nm); and (c) polymer **P3** : $PC_{71}BM$ 1 : 1 blend (rms = 1.22 nm); scan size (5 µm × 5 µm).

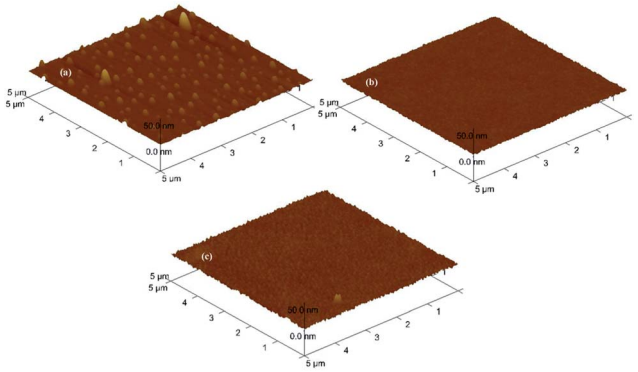

**Fig. 3** 3D TMAFM phase images of the solar cell devices with 3% DIO: (a) polymer **P1** : $PC_{71}BM$ = 1 : 1blend (rms-2.08); (b) polymer **P2** : $PC_{71}BM$ = 1 : 1 blend (rms = 0.88); and (c) polymer **P3** : $PC_{71}BM$ = 1 : 1 blend (rms = 1.24 nm); scan size (5 μm × 5 μm).

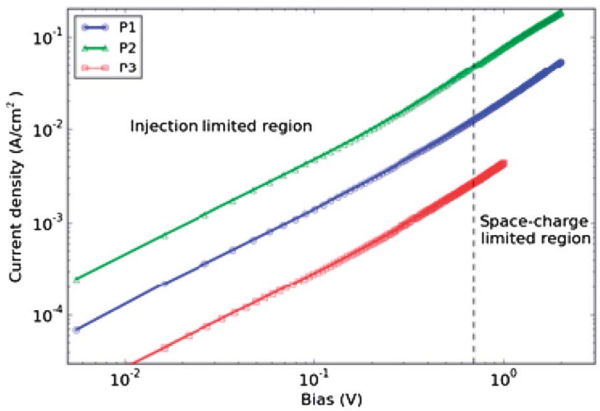


**Fig. 4** Current density and voltage curves of polymer **P1**, **P2**, and **P3**.

roughness (rms = 2.08 nm), which contributed to the poor device performance (Fig. 3, S27 and S28 in ESI†).

### 3.7. Space charge limited current studies

To investigate the vertical hole-carrier transport behaviour of the reported polymers, the space charge limited current (SCLC) model was employed using the following equation:

$$J = 9\varepsilon_0\varepsilon_r\mu\frac{V^2}{8L^3}$$

where $J$ is the current density, $\varepsilon_0\varepsilon_r$ is the permittivity of the polymer, $\mu$ is the charge carrier mobility, and $L$ is the active layer thickness.

A device structure of ITO/PEDOT:PSS/polymer/Al was employed and the mobilities were extracted in the SCLC region. The Fig. 4 shows the current density and voltage curves for the reported polymers. Polymer **P2** showed the highest charge carrier mobility of $8.71 \times 10^{-5}$ $cm^2$ $V^{-1}$ $s^{-1}$. Polymer **P3** had a charge carrier mobility of $4.54 \times 10^{-5}$ $cm^2$ $V^{-1}s^{-1}$, while polymer **P1** had the lowest charge carrier mobility of $1.33 \times 10^{-5}$ $cm^2$ $V^{-1}$ $s^{-1}$. These measured mobilities are consistent with the solar cell data, in which the highest PCE was obtained by the polymer **P2** due to its larger short circuit current density.

## 4. Conclusion

Three new donor–acceptor copolymers **P1**, **P2** and **P3** were synthesized by Stille coupling polymerization with bis(bithienyl)- substituted BDT as the donor and 5,6-difluorobenzo[*c*]-[1,2,5]thiadiazole, 4,7-di(thiophen-2-yl)benzo[*c*][1,2,5]thiadiazole and 5,6-difluoro-4,7-di(thiophen-2-yl)benzo[*c*][1,2,5]thiadiazole as the acceptor units, respectively. The polymers had comparable molecular weights ($M_n \sim 20\,000$ g $mol^{-1}$) and they had good solubility in common organic solvents. The insertion of the thiophene spacer between the donor and the acceptor units broadened the absorption spectrum of the polymers **P2** and **P3** as compared to polymer **P1**. Moreover, polymers **P2** and **P3** showed a larger red shift in the UV/vis spectrum indicating better solid state packing and improved the conjugation which was beneficial for the charge transport. The attachment of the fluorine atoms on the acceptor had an adverse effect on the photovoltaic properties of the polymers, most likely because the electron withdrawing fluorine deepened the HOMO level of the polymer, which in turn increased the band gap of the polymer and consequently resulted in lower $J_{SC}$ in the BHJ solar cells. Polymer **P2** had the highest charge carrier mobility of $8.71 \times 10^{-5}$ $cm^2$ $V^{-1}$ $s^{-1}$ as determined by SCLC method and gave the highest PCE of 3.52% in BHJ with $PC_{71}BM$ acceptor.

## Acknowledgements

Financial support for this project from NSF (Career DMR-0956116) and Welch Foundation (AT-1740) is gratefully acknowledged. We gratefully acknowledge the NSF-MRI grant (CHE-1126177) used to purchase the Bruker Avance III 500 NMR instrument.

## Notes and references

1 Z. He, C. Zhong, S. Su, M. Xu, H. Wu and Y. Cao, *Nat. Photonics*, 2012, **6**, 591–595.
2 I. F. Perepichka and D. F. Perepichka, *Handbook of Thiophene-based Materials: Applications in Organic Electronics and Photonics, Volume One: Synthesis and Theory*, 2009.
3 J. Chen and Y. Cao, *Acc. Chem. Res.*, 2009, **42**, 1709–1718.
4 Y. Liang, D. Feng, Y. Wu, S.-T. Tsai, G. Li, C. Ray and L. Yu, *J. Am. Chem. Soc.*, 2009, **131**, 7792–7799.
5 J. Hou, H.-Y. Chen, S. Zhang, R. I. Chen, Y. Yang, Y. Wu and G. Li, *J. Am. Chem. Soc.*, 2009, **131**, 15586–15587.
6 F. Huang, K.-S. Chen, H.-L. Yip, S. K. Hau, O. Acton, Y. Zhang, J. Luo and A. K. Y. Jen, *J. Am. Chem. Soc.*, 2009, **131**, 13886–13887.
7 R. S. Kularatne, H. D. Magurudeniya, P. Sista, M. C. Biewer and M. C. Stefan, *J. Polym. Sci., Part A: Polym. Chem.*, 2012, **51**, 743–768.
8 H. Pan, Y. Li, Y. Wu, P. Liu, B. S. Ong, S. Zhu and G. Xu, *Chem. Mater.*, 2006, **18**, 3237–3241.

 

9 J. Hou, M.-H. Park, S. Zhang, Y. Yao, L.-M. Chen, J.-H. Li and Y. Yang, *Macromolecules*, 2008, **41**, 6012–6018.
10 P. Sista, J. Hao, S. Elkassih, E. E. Sheina, M. C. Biewer, B. G. Janesko and M. C. Stefan, *J. Polym. Sci., Part A: Polym. Chem.*, 2011, **49**, 4172–4179.
11 P. Sista, R. S. Kularatne, M. E. Mulholland, M. Wilson, N. Holmes, X. Zhou, P. C. Dastoor, W. Belcher, S. C. Rasmussen, M. C. Biewer and M. C. Stefan, *J. Polym. Sci., Part A: Polym. Chem.*, 2013, **51**, 2622–2630.
12 P. Sista, B. Xue, M. Wilson, N. Holmes, R. S. Kularatne, H. Nguyen, P. C. Dastoor, W. Belcher, K. Poole, B. G. Janesko, M. C. Biewer and M. C. Stefan, *Macromolecules*, 2012, **45**, 772–780.
13 N. Hundt, K. Palaniappan, J. Servello, D. K. Dei, M. C. Stefan and M. C. Biewer, *Org. Lett.*, 2009, **11**, 4422–4425.
14 Y. He, Y. Zhou, G. Zhao, J. Min, X. Guo, B. Zhang, M. Zhang, J. Zhang, Y. Li, F. Zhang and O. Inganaes, *J. Polym. Sci., Part A: Polym. Chem.*, 2010, **48**, 1822–1829.
15 S. C. Price, A. C. Stuart, L. Yang, H. Zhou and W. You, *J. Am. Chem. Soc.*, 2011, **133**, 4625–4631.
16 Y. Liang, Z. Xu, J. Xia, S.-T. Tsai, Y. Wu, G. Li, C. Ray and L. Yu, *Adv. Mater.*, 2010, **22**, E135–E138.
17 P. Sista, H. Nguyen, J. W. Murphy, J. Hao, D. K. Dei, K. Palaniappan, J. Servello, R. S. Kularatne, B. E. Gnade, B. Xue, P. C. Dastoor, M. C. Biewer and M. C. Stefan, *Macromolecules*, 2010, **43**, 8063–8070.
18 R. S. Kularatne, P. Sista, H. Q. Nguyen, M. P. Bhatt, M. C. Biewer and M. C. Stefan, *Macromolecules*, 2012, **45**, 7855–7862.
19 H. Zhou, L. Yang, S. Xiao, S. Liu and W. You, *Macromolecules*, 2009, **43**, 811–820.
20 D. Mühlbacher, M. Scharber, M. Morana, Z. Zhu, D. Waller, R. Gaudiana and C. Brabec, *Adv. Mater.*, 2006, **18**, 2884–2889.
21 J. Peet, J. Y. Kim, N. E. Coates, W. L. Ma, D. Moses, A. J. Heeger and G. C. Bazan, *Nat. Mater.*, 2007, **6**, 497–500.
22 F. Zhang, K. G. Jespersen, C. Björström, M. Svensson, M. R. Andersson, V. Sundström, K. Magnusson, E. Moons, A. Yartsev and O. Inganäs, *Adv. Funct. Mater.*, 2006, **16**, 667–674.
23 L. M. Andersson, Z. Fengling and I. Olle, *Appl. Phys. Lett.*, 2007, **91**, 071108.
24 L. H. Slooff, S. C. Veenstra, J. M. Kroon, D. J. D. Moet, J. Sweelssen and M. M. Koetse, *Appl. Phys. Lett.*, 2007, **90**, 143506.
25 C. J. Brabec, C. Winder, N. S. Sariciftci, J. C. Hummelen, A. Dhanabalan, P. A. van Hal and R. A. J. Janssen, *Adv. Funct. Mater.*, 2002, **12**, 709–712.
26 J. R. Tumbleston, A. C. Stuart, E. Gann, W. You and H. Ade, *Adv. Funct. Mater.*, 2013, **23**, 3463–3470.
27 C.-P. Chen, Y.-C. Chen and C.-Y. Yu, *Polym. Chem.*, 2013, **4**, 1161–1166.
28 Y. Zhang, S.-C. Chien, K.-S. Chen, H.-L. Yip, Y. Sun, J. A. Davies, F.-C. Chen and A. K. Y. Jen, *Chem. Commun.*, 2011, **47**, 11026–11028.
29 H. Bronstein, J. M. Frost, A. Hadipour, Y. Kim, C. B. Nielsen, R. S. Ashraf, B. P. Rand, S. Watkins and I. McCulloch, *Chem. Mater.*, 2013, **25**, 277–285.
30 H. Zhou, L. Yang, A. C. Stuart, S. C. Price, S. Liu and W. You, *Angew. Chem., Int. Ed.*, 2011, **50**, 2995–2998.
31 F. Wu, D. Zha, L. Chen and Y. Chen, *J. Polym. Sci., Part A: Polym. Chem.*, 2013, **51**, 1506–1511.
32 P. M. Beaujuge, C. M. Amb and J. R. Reynolds, *Acc. Chem. Res.*, 2010, **43**, 1396–1407.
33 Y. Zou, A. Najari, P. Berrouard, S. Beaupre, A. B. Reda, Y. Tao and M. Leclerc, *J. Am. Chem. Soc.*, 2010, **132**, 5330–5331.
34 P. J. Brown, D. S. Thomas, A. Kohler, J. S. Wilson, J.-S. Kim, C. M. Ramsdale, H. Sirringhaus and R. H. Friend, *Phys. Rev. B: Condens. Matter Mater. Phys.*, 2003, **67**, 064203.
35 Y. Sun, S.-C. Chien, H.-L. Yip, Y. Zhang, K.-S. Chen, D. F. Zeigler, F.-C. Chen, B. Lin and A. K. Y. Jen, *J. Mater. Chem.*, 2011, **21**, 13247–13255.
36 L. D. M. de, M. M. J. Simenon, A. R. Brown and R. E. F. Einerhand, *Synth. Met.*, 1997, **87**, 53–59.
37 B. C. Thompson, Y.-G. Kim and J. R. Reynolds, *Macromolecules*, 2005, **38**, 5359–5362.
38 J. K. Lee, W. L. Ma, C. J. Brabec, J. Yuen, J. S. Moon, J. Y. Kim, K. Lee, G. C. Bazan and A. J. Heeger, *J. Am. Chem. Soc.*, 2008, **130**, 3619–3623.
39 Y. Huang, X. Guo, F. Liu, L. Huo, Y. Chen, T. P. Russell, C. C. Han, Y. Li and J. Hou, *Adv. Mater.*, 2012, **24**, 3383–3389.
40 L. Huo, S. Zhang, X. Guo, F. Xu, Y. Li and J. Hou, *Angew. Chem., Int. Ed.*, 2011, **50**, 9697–9702.
41 B. R. Aich, J. Lu, S. Beaupre, M. Leclerc and Y. Tao, *Org. Electron.*, 2012, **13**, 1736–1741.
42 H. G. Kim, S. B. Jo, C. Shim, J. Lee, J. Shin, E. C. Cho, S.-G. Ihn, Y. S. Choi, Y. Kim and K. Cho, *J. Mater. Chem.*, 2012, **22**, 17709–17717.
43 G. Ren, E. Ahmed and S. A. Jenekhe, *Adv. Energy Mater.*, 2011, **1**, 946–953.
44 H. Hoppe and N. S. Sariciftci, *J. Mater. Chem.*, 2006, **16**, 45–61.